Charge Separation Process in Water Clusters Containing HCl. Molecular Dynamics Study Using Semiempirical Hamiltonians

Oscar Ivan Arillo Flores and Margarita I. Bernal-Uruchurtu*

Centro de Investigaciones Químicas, Universidad Autónoma del Estado de Morelos, Cuernavaca, Morelos 62209, Mexico

Received: February 28, 2010; Revised Manuscript Received: July 12, 2010

The acid dissociation of HCl in water clusters was studied using the PM3-MAIS model in a direct molecular dynamic simulations framework. Several trajectories for each cluster size were computed to improve the sampling on the potential energy surface and to increase the statistical significance of our study. We have analyzed the emergence of well-defined hydration structures around the ions and the effect they have on the charge separation process. Surface and bulk solvation situations are examined for both ions in terms of the competing circumstances for water molecules in the cluster. Our results show that the prevailing situation in all these clusters is a water mediated interaction between the ions. This situation is related to the significant interplay of several factors such as charge transfer occurring between the ions and their first hydration shells. Our results show that no significant charge redistribution occurs during the Eigen−Zundel transformation.

I. Introduction

Molecular clusters have been considered as model systems for a wide variety of phenomena occurring in condensed phases. Due to their size, they provide an excellent model for developing a detailed description of molecular processes from chemical reactions to solvent effects. With the advent of refined experimental techniques to produce and analyze molecular clusters,[1,2] these systems have become a fast-growing research area as a consequence of their relevance in different areas of chemistry. Ionic water clusters are the most ubiquitous clusters present in the atmosphere:[3] they are involved in processes ranging from weather regulation to fundamental phenomena such as nucleation,[4] heterogeneous reactions,[5,6] and energy transfer processes.[7] In this work we focus our attention on the ionic hydration process that eventually leads to charge separation after the acid dissociation reaction takes place. This process can be thought of as the gradual generation of independent hydration shells around each ion with intermediate stages consisting, first, in a contact ion pair (CIP) that evolves to a solvent separated ionic pair (SSIP). It is expected that, in the clusters, the reduced number of water molecules strongly influences the degree of charge separation.

The behavior of the cation H^+ has been extensively studied in the past. It is known that its presence has a profound impact on the phase transition of small clusters in atmospheric conditions;[2] its diffusion mechanism has been thoroughly studied and the role of solvating molecules in it is now well-defined.[2,8−15] Over the years, the controversy on the nature of the hydrated proton has evolved to a point in which both cationic forms H_3O^+ and $H_5O_2^+$ or Zundel ion[16] have been recognized as limit structures of a very fluxional system. In particular, the hydronium ion, as the core of the Eigen complex ($H_9O_4^+$),[17] seems to have a very small probability of appearing in solution,[18,19] but under special conditions its presence can be detected.[15]

On the other hand, halides had been an excellent probe of the different modern methodologies used to study aqueous systems. Ab initio calculations[20,21] and experimental studies of halides in water clusters[22−25] as well as molecular simulations of solutions[26] have slowly converged to a picture of halide solvation in which their polarizability plays a very important role.[27−32]

There is a fair amount of theoretical information regarding the behavior of ions in clusters, in particular protons in aqueous environments where no counterion was considered. In this work we can also look at the effect the presence of an anion in the cluster has on the proton structural and dynamic properties and vice versa. In the case of ions with opposite charge it is also of interest to describe how the known differences between cation and anion hydration preferences affect the global cluster structure and ionic separation, characteristics both important to portraying the fundamental dissociation process. After the acid dissociation reaction takes place, solvent reorganization is a crucial factor in determining the relative stability between the contact ion pair (CIP) and the solvent separated ion pair (SSIP), configurations that in general terms can be considered as a measure of the degree of charge separation. The relative stability between the SSIP situation and CIP is crucially dependent on the form in which water molecules are structured around each ion and, at the same time, on the way they bond each other to maintain the cluster integrity. These characteristics are dependent on factors such as temperature, pressure, and not surprisingly the aggregate size. Simulation results point out that, within the relevant conditions for aqueous clusters, the increase in the number of solvent molecules has a larger stabilization effect on the SSIP than raising the system temperature.[4,33]

The HCl dissociation process has been theoretically and experimentally studied in almost every possibly imaginable aqueous system.[6,34−47] Most of these works dealt with the initial stages of the reaction in such a way that the number of molecules involved in the process, their relative orientation, and the solvation effects are well-known. However, the evolution of the ionic products in the system has not yet received as much attention. Using semiempirical Born−Oppenheimer molecular dynamics calculations, we follow the process in clusters ranging from 6 to 21 water molecules. The moderate computational cost

* To whom correspondence should be addressed. E-mail: mabel@uaem.mx.

10.1021/jp101803r
Published on Web 08/02/2010

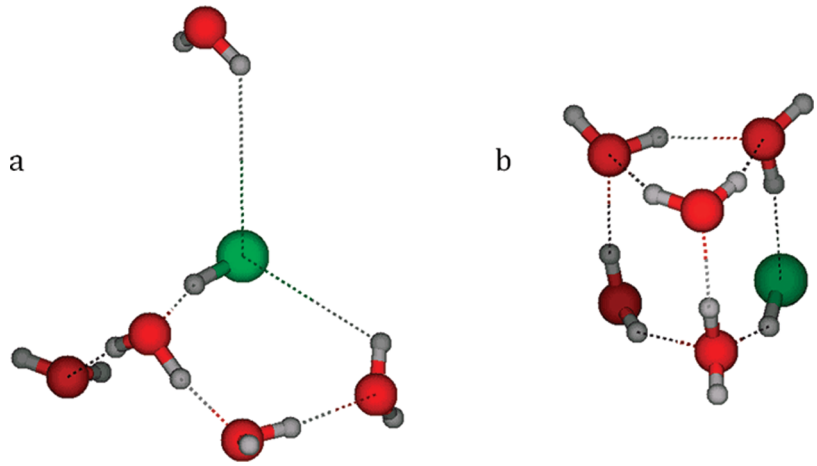

Figure 1. Fragments of initial geometries of clusters (a) with the structural motif that promotes HCl dissociation and (b) in which the dissociation occurs after 10 ps.

of this method enabled the collection of a large amount of information about the system, ensuring a proper sampling of its potential energy surface. Our results clearly show that ions do not achieve independent solvation in this cluster size range. The reasons behind this finding are explored using the semiempirical wave function of the entire cluster. We present the results of this study in sections corresponding to the different stages of the process occurring in the clusters: the acid dissociation and the identification of the products, the hydration of the products, and the dynamics of the ions in the clusters. Our results raise a recurrent question in the field: how many molecules are required to reproduce the bulk behavior of solutions?[48,49] It is possible that within this size range we are able to provide a molecular understanding of concentrated HCl solutions.

II. Methodology

In a recent work we reported the PM3-MAIS parameters to describe the dissociated and nondissociated structures of $HCl(H_2O)_n$ clusters.[50] The interaction energies and geometric parameters of dissociated structures obtained with PM3-MAIS are in good agreement with those coming from ab initio methods. These results, combined with the affordable computational cost of the semiempirical calculations, have attracted interest for applications to elemental reactive processes by numerical simulations.[51] Using this PM3-MAIS model, we performed direct molecular dynamics (MD) simulations of $HCl(H_2O)_n$ clusters with $n = 6, 7, 8, 10, 12, 15, 17, 19, 20$, and 21; for $Cl^-(H_2O)_{10\text{ and }21}$; and for $H^+(H_2O)_{10\text{ and }21}$. No restrictions were imposed on the geometry, and in each MD step a semiempirical self-consistent field (SCF) calculation of the whole system was performed using standard techniques for the full Fock matrix diagonalization. The molecular dynamics code was coupled with the GEOMOS package,[52] and the classical equations of motion were integrated employing the velocity Verlet algorithm[53] with a simulation step of 0.2 fs. The cluster trajectories were obtained in a constant energy ensemble whose equilibrium condition was verified confirming that a Maxwell−Boltzmann distribution of velocities was reached and that the total energy fluctuations were <5%. Being gas phase simulations, the volume was not kept constant and the estimated fluctuations of this property were observed to be <16%. Evaporation of water molecules was an event rarely observed, and in the few cases it happened the entire trajectory was discarded from the analysis. All simulations were done using a constant total energy criterion, and velocities were scaled to keep the kinetic temperature at fixed values of 100 and 200 K.

Several trajectories for each neutral cluster size were computed to improve the sampling on the potential energy surface and increase the statistical significance of our study. For clusters in the range $n = 6-10$ an average of 9.5 trajectories of 80 ps were calculated. For the larger clusters 14 trajectories of 33 ps each were computed on average. Consequently, the total production time subject to analysis amounts to 5.8 ns. For the ionic clusters with H^+ or Cl^-, an average of seven trajectories were obtained totaling ca. 200 ps for each ion.

The starting geometries used for each trajectory were selected or built in three different manners: some of them correspond to previously reported stationary structures for $HCl:H_2O$ clusters,[40] or modified neutral water clusters,[54] or protonated water clusters[55] to which HCl or Cl^- was added. With the aim of reducing the discrete size defects on the studied properties, the final geometric configurations of some trajectories from the $HCl(H_2O)_m$ cluster were used as starting geometries for trajectories of the $HCl(H_2O)_{m+1}$ and $HCl(H_2O)_{m+1}$ aggregates. During the production time, nuclear position coordinates and velocities were collected at 10 fs intervals; this time resolution is sufficient for the observation of the fast proton transfer process.[8,56]

III. Results and Discussion

A. HCl Dissociation in Water Clusters. The active role water molecules play in the dissociation mechanisms of different acids is driven by specific molecular interactions as has been thoroughly recognized.[34,36] In the clusters we studied, the coordination of HCl to water network completely determined the time required for dissociation to occur. In Figure 1 we present two examples of coordination motifs present in the initial geometries of the studied clusters: case a corresponds to an arrangement in which the chlorine atom accepts at least two hydrogen bonds and the acidic proton donates to a water molecule that is already a double hydrogen bond donor (dd); case b differs from the previous one in the basicity of the accepting water molecule. We observed that for the MD trajectories starting with cluster geometries containing motif a (Figure 1a) HCl dissociation occurred in 0.55 ± 0.47 ps and this time is not dependent on the number of molecules in the cluster, whereas for the other case (Figure 1b), the time required was ~10 ps, considerably longer than the average lifetime of a hydrogen bond (1−3.5 ps)[57] or the rotation of a water molecule (2 ps),[58] confirming that more than one of these events takes place during the structural rearrangement of the cluster prior to dissociation. The dissociation process is considered complete when one of the protonic forms of water, H_3O^+ or $H_5O_2^+$, is

TABLE 1: PM3-MAIS Molecular Dynamics Derived Solvation Properties of Individual Ions H^+ and Cl^- in 10 and 21 Water Molecule Clusters at 100 K[a]

	first solvation shell				second solvation shell			
	N		*R* (Å)		*N*		*R* (Å)	
ion	$[ion(H_2O)_{10}]$	$[ion(H_2O)_{21}]$	$[ion(H_2O)_{10}]$	$[ion(H_2O)_{21}]$	$[ion(H_2O)_{10}]$	$[ion(H_2O)_{21}]$	$[ion(H_2O)_{10}]$	$[ion(H_2O)_{21}]$
H_3O^+	3.0 ± 0.0	3.0 ± 0.0	2.49 ± 0.01	2.50 ± 0.03	4.4 ± 0.5	6.0 ± 0.2	4.16 ± 0.08	4.15 ± 0.08
$H_5O_2^+$	3.8 ± 0.3	4.0 ± 0.1	2.59 ± 0.01	2.58 ± 0.02	5.7 ± 0.8	7.5 ± 0.9	4.15 ± 0.17	4.23 ± 0.15
Cl^-	3.1 ± 0.6	4.1 ± 0.5	3.05 ± 0.04	3.11 ± 0.03	3.4 ± 0.6	5.9 ± 0.1	4.32 ± 0.13	4.38 ± 0.13

[a] *N* is the number of water molecules in each solvation shell, and *R* is the average distance of these molecules to the ion.

detected. The coordination requirements leading to a fast dissociation process are found to be the same for HCl dissociation on ice and at the air−water interface.[6,45,46,59] Once the relevance of this pattern was confirmed for the dissociation occurring in the clusters and with the purpose of obtaining long trajectories, several of the initial configurations used in this study were built with matching characteristics.

The definition of the H_3O^+ cation we used is an oxygen atom with three neighboring hydrogen atoms at distances of ≤1.11 Å, and the $H_5O_2^+$ cation is defined as two oxygen atoms at a distance of ≤2.45 Å and a hydrogen atom with distances to both oxygens no greater than 1.26 Å. For this latter ion, we considered an additional criterion: the angle O−H−O with values of ≥174°. The given values for these criteria were initially based on the averages and fluctuations of corresponding geometric parameters measured on individual trajectories of the isolated cations simulated at 298 K during 100 ps. These values are in close agreement with the definition used by Sillanpää and Laasonen in their study of concentrated HCl solutions.[47] However, the precise values employed in this work were carefully adjusted to provide the highest detection while ensuring mutual exclusion between the two protonic forms. Due to intermolecular vibration and deformation of the molecules these criteria are not fulfilled all the time; thus, the detection levels attained values ranging from 40 to 60% of the total geometric configurations analyzed in each trajectory. As previously suggested,[60] on the remnant of the trajectory the protonic defect may be identified as a deformed H_3O^+ or $H_5O_2^+$ ion, confirming that these structures are limiting geometries of a highly fluxional complex.[9]

B. Structural Aspects on the Ions and Their Solvation Shells. The criteria we used to identify the solvation shells are based on the structural characteristics found on the radial distribution functions obtained for the $HCl(H_2O)_{20}$ system on 400 ps of MD PM3-MAIS over 10 trajectories (included as Supporting Information). For the cations the criteria can be summarized as follows: water molecules in the first coordination shell of H_3O^+ or $H_5O_2^+$ cations are those whose oxygens are ≤3.0 Å from the oxygen atom of the protonated molecule; second shell molecules are those whose oxygen atoms are also at distances of ≤3.0 Å from the oxygen atom of any water molecule in the first shell. Hydrogen bonding between the first shell molecules and the cation was confirmed with H-bond distances of ≤2.1 Å. For the anion, water molecules in the first coordination shell are those whose oxygen atoms are at a distance of ≤3.8 Å and one of their hydrogen atoms is placed at a distance of ≤2.5 Å of the Cl^-. Second shell molecules around chloride are defined as for the cation. On the analysis of the coordination numbers around each ion, it is important to remember that the formation of the $H_5O_2^+$ ion requires one more water molecule than H_3O^+; this difference has direct consequences on the number of available water molecules for ionic solvation in the cluster. However, the results are discussed in terms of the total number of water molecules in the system.

Ionic solvation in clusters has been a thoroughly studied subject, and there is a vast amount of theoretical and experimental information about protonated clusters and chloride clusters. In our case, we have a neutral system in which the counterion effects are expected to be relevant to the charge separation process. To clearly distinguish these effects from the methodology used, we obtained MD trajectories of a small cluster and a midsize cluster (10 and 21 water molecules) with a single ion. The 21 water molecule clusters are large enough to provide a complete solvation for both ions.[21] The coordination numbers in the first and second solvation shells of each ion and their average positions are gathered in Table 1. For the protonated ions the coordination numbers and the positions of the first shells are in agreement with what is obtained from diffraction experiments of concentrated HCl solutions and protonated cluster calculations.[43,55,61−63] Furthermore, no axial coordination was observed for the cation since the protonic defect is a good hydrogen bond donor but a bad acceptor. On the other hand, diffraction experiments of chloride-containing solutions point to a coordination number closer to six water molecules in which some overlap with a second hydration shell was observed.[64] The value we obtain is below the experimental average (5.5−6) for solutions but is in reasonably good agreement with what has been found for solvation in clusters.[26,65]

For the neutral systems, the average coordination numbers around H_3O^+ and $H_5O_2^+$ were obtained for each cluster size using the information of all the calculated trajectories at a given temperature. As shown in Figure 2a, the H_3O^+ cation completes its first shell with three molecules even for the smallest studied systems ($n = 6-8$), thus confirming the presence of the Eigen complex.[17] This is not the case for the $H_5O_2^+$ ion, which has an average coordination number of 3.0 within the same size range and attains a complete first shell in bigger clusters, $n = 10$. This difference is related to the *effective* number of water molecules available in the cluster, but it is also an indication of the different interaction between the cationic moieties and the water molecules around them. Another significant difference between H_3O^+ and $H_5O_2^+$ ions is the size of the fluctuations around the average coordination number. The hydronium ion consolidates its first solvation shell quite consistently, leading to the Eigen complex ($H_9O_4^+$). Interestingly, the size of the fluctuations on the number of water molecules that surround this complex (second shell molecules around H_3O^+) is also smaller than what is observed for the Zundel form. For the clusters in the range $n = 8-12$ it can be observed that the rate of incorporation of water molecules to their hydration structures is different for both protonic forms: the Eigen complex gets ∼75% of its coordination in this range whereas the Zundel form only gets ∼63%. This trend changes after $n = 12$: the solvation around $H_5O_2^+$ grows slightly faster than that for the Eigen complex. In fact, taking into account the existence of a significant second hydration shell around the cation, it is possible to divide the studied systems into two subsets: small clusters with $n \leq 12$ water molecules and medium-sized clusters with

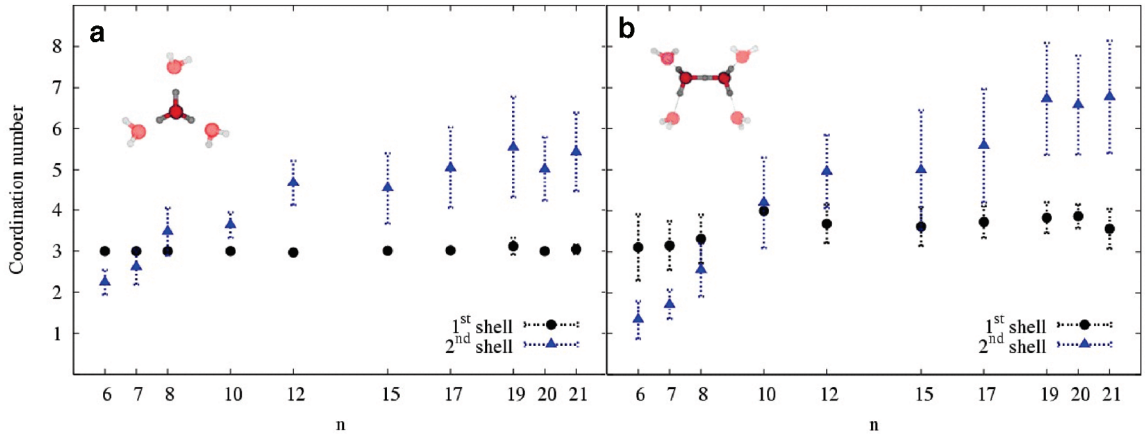

Figure 2. Average coordination numbers in (a) first and (b) second solvation shells of both protonic forms in $HCl(H_2O)_n$ clusters.

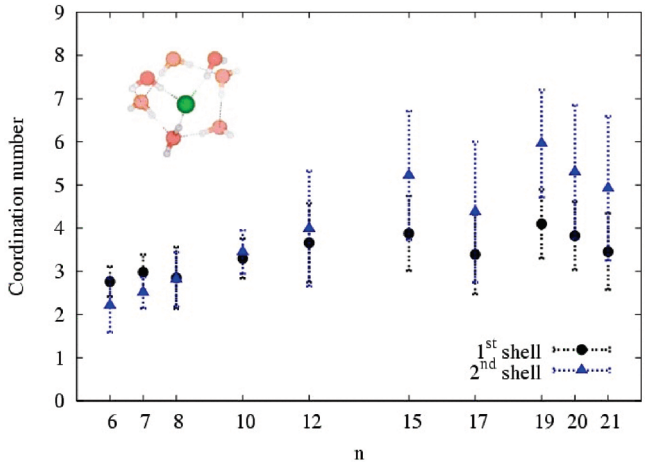

Figure 3. Average coordination numbers in first and second solvation shells of chloride in $HCl(H_2O)_n$ clusters.

$n > 12$. For the largest systems studied, $n = 15-21$, there are enough water molecules in the cluster to generate more defined second hydration shells around the cations. For $n = 21$, the Eigen form has 5.4 molecules around it and the Zundel form has 6.8 in both cases, close to the corresponding saturation values of 6 and 8 molecules, respectively. It is worth mentioning that one of the reasons leading to the production of several trajectories was the fact that no convergent behavior on the coordination numbers was obtained when a small set was used (<10). This stresses the relevance of a thorough sampling of the potential energy surface for these systems.

The average coordination numbers for Cl^- in the clusters are shown in Figure 3. The growth of the hydration shells around the anion does not exhibit the trend observed for the cations, but the fluctuations around the average coordination numbers are the same size as those observed for the protonic moieties. Again, this equivalence was only reached when a large number of trajectories were taken into account. The maximum hydration numbers are reached for $n \geq 15$: about four water molecules in the first shell and six in the second one.

Data in Table 2 allow examining the main differences in the hydration structures around the ions in neutral and charged clusters. As expected, coordination numbers in the neutral systems are smaller than those found for the ionic clusters; the Zundel and the chloride ion are the most affected since the hydronium ion forms the Eigen complex quite consistently.

It is very interesting that albeit the limited size of the studied systems these results are in close agreement what has been found in the study of HCl concentrated solutions (1:9 solution of HCl) by neutron diffraction experiments, where 4.4 ± 1.4 water molecules are placed around each Cl^- ion.[39] The large uncertainty associated with the average coordination number was associated with the incomplete acid dissociation. Considering that in these clusters we explore a concentration range similar to the one used in the diffraction experiments, it is possible to think that the uncertainty observed can also be due to the presence of H^+ ions in the vicinity of the anion. However, the fact that for clusters with smaller acid/water ratio the size of the hydration structure is not significantly augmented deserves a more detailed analysis. There are plausible reasons that might be related to this situation: (1) the energetic preference of water molecules to solvate the cation or to incorporate to a discrete motif on the water network and (2) the placement of the anion near the surface of the cluster, an external solvation structure.

The ease of each ion for structuring the solvent around it can be partially understood in terms of the pair interaction energies of several complexes. PM3-MAIS predicts that the interaction of a single water molecule with H_3O^+ is 14 kcal/mol stronger than with a Zundel cation,[66] concurring with recent calculations[67] and explaining why the H_3O^+ cation is the first ion completing its first hydration shell. The addition of a water molecule to the Eigen complex is almost twice (1.7 times) as favorable as doing so to an equivalent water cluster (13.1 vs 4.9 kcal/mol). This energetic preference results in an interesting situation: incorporating water molecules to the second shell of the cation is almost equivalent to their inclusion in the first shell around the chloride ion. Therefore, inside this cluster size interval, the cation is more efficacious for organizing solvent molecules around it while the hydration of chloride depends primarily on the global cluster structure.

Not all water molecules in the cluster form part of the solvation shells of the ions. This is reflected in the formation of a more structured and extended hydrogen bond network with well-defined motifs such as the examples shown in Figure 4. The smaller clusters form rings and small cages (Figure 4a) in contrast to what has been observed for protonated water systems in which the cage motif is the dominant structure for clusters with $n \geq 11$.[68] For the systems with $n = 10$ and 12, fused rings and cage structures are observed (Figure 4b) and coincide with the size increase of the second solvation shell of the cationic moieties. Larger cages and distorted prismatic structures characterize clusters with $n = 15$ (Figure 4c), and clathrate-like geometries appear within the range $n = 19-21$ as shown in Figure 5. The formation of this type of structure is induced by the coordination motifs the protonic moiety induces in the

TABLE 2: Selected PM3-MAIS Molecular Dynamics Derived Solvation Properties of the Ionic Species Present in HCl−(H_2O) Clusters at 100 K[a]

	first solvation shell				second solvation shell			
	N		*R* (Å)		*N*		*R* (Å)	
ion	$[HCl(H_2O)_{10}]$	$[HCl(H_2O)_{21}]$	$[HCl(H_2O)_{10}]$	$[HCl(H_2O)_{21}]$	$[HCl(H_2O)_{10}]$	$[HCl(H_2O)_{21}]$	$[HCl(H_2O)_{10}]$	$[HCl(H_2O)_{21}]$
H_3O^+	3.0 ± 0.0	3.0 ± 0.0	2.48 ± 0.01	2.48 ± 0.01	3.6 ± 0.3	5.4 ± 0.1	4.12 ± 0.03	4.15 ± 0.03
$H_5O_2^+$	4.0 ± 0.0	3.6 ± 0.5	2.57 ± 0.01	2.57 ± 0.01	4.2 ± 1.1	6.8 ± 0.4	4.16 ± 0.02	4.17 ± 0.02
Cl^-	3.3 ± 0.5	3.5 ± 0.9	3.04 ± 0.02	3.08 ± 0.02	3.5 ± 0.5	4.9 ± 1.7	4.19 ± 0.04	4.24 ± 0.04

[a] *N* is the number of water molecules in each solvation shell, and *R* is the average distance of these molecules to the ion.

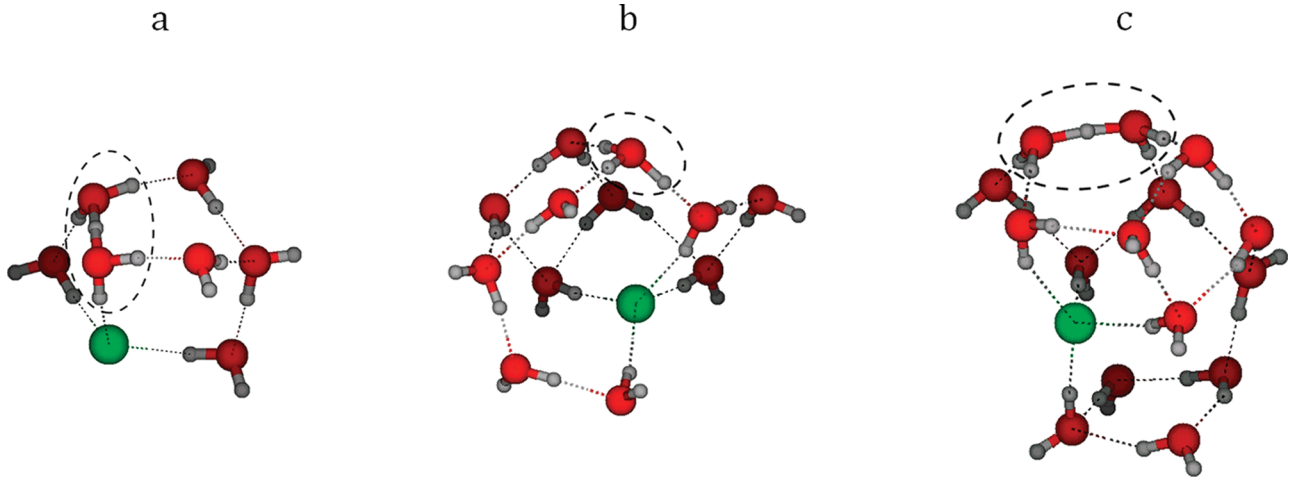

Figure 4. Snapshot of $HCl(H_2O)_n$ clusters containing (a) a small cage, (b), fused rings, and (c) distorted prism motifs in their structures.The cationic form is encircled for clarity.

solvent molecules around it.[2,68,69] Moreover, the Eigen complex is usually found at the top of pyramid-like structures, whereas due to its flexibility the Zundel ion adapts to a large variety of H-bonded patterns. It is possible to think that this difference might result in an entropic advantage for the presence of $H_5O_2^+$ in aqueous systems.

The formation of stable and long-lived ring structures also leads to H-bonded motifs that are not very effective for ionic hydration. In these patterns the non-H-bonded atoms point outward from the structure; thus, they are not available to interact with the ions. The emergence of a more structured hydrogen bond network has a more acute effect on chloride solvation than on the cations. The structures presented in Figure 5 exemplify this situation. In Figure 5b the chloride ion is placed at the vertex of several fused rings, an ideal position for solvation, whereas in Figure 5a,c, its placement near the surface of the cluster or in the center of nest-like cavities leads to a reduced solvation number. As recently suggested by Wick and Xantheas,[32] the polarizability of the anion is behind the anisotropic solvation environment that surrounds them. In condensed phases this leads to an enhanced interfacial activity, and as we found, in medium-sized clusters this promotes the formation of cavities. It is important to keep in mind that in our work polarizability is limited by the fact that semiempirical methods use a minimal basis set.

Furthermore, these findings resemble what Lagutschenkov et al.[70] showed for water clusters: a transitional size regime where preferential stabilization alternates between "all-surface" and "internally solvated" configurations. However, a definite assessment of a structural transition in the systems $HCl(H_2O)_n$ or $Cl^-(H_2O)_n$ would require a more systematic study of these clusters (all values of *n*). Moreover, low coordination and surface position of chloride have also been found in numerical simulations of $Cl^-(H_2O)_{17}$ aggregates where box-shaped structures were commonly found.[63]

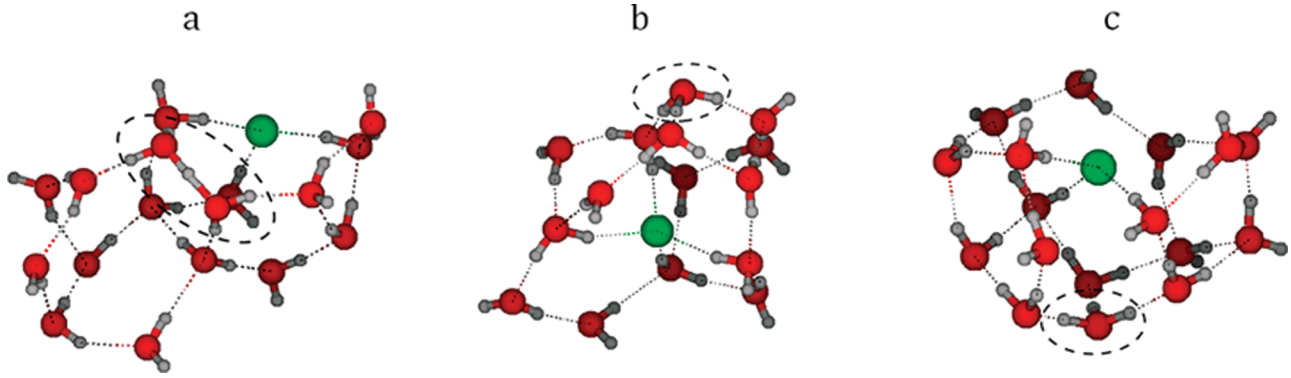

Figure 5. Instant geometries found in trajectories of $HCl(H_2O)_n$ clusters with (a, c) $n = 17$ and (b) $n = 15$.

For the systems $H^+(H_2O)_n$ it has been observed that an increase in temperature from 100 to 200 K promotes the opening of rings and cages to form chains, branched structures, and fused rings.[61] In this work, the cluster geometries of $HCl(H_2O)_n$ coming from trajectories at 100 K do not exhibit relevant differences from those obtained at 200 K. However, the increase in kinetic energy content has a small effect on the hydration shells around the protonic ions and chloride; their average coordination numbers in second shells are reduced in average by 0.5−1.0 molecule whereas there is not an appreciable change in their first shells. The fact that both ions lower their coordination numbers suggests that some water molecules migrate to the incipient water network.

The first hydration shell around the two protonic moieties is placed at different average distances, 2.48 ± 0.01 and 2.57 ± 0.01 Å for the H_3O^+ and $H_5O_2^+$ ions, respectively. This difference is related to the charge/radius ratio of the cations. Both values are slightly shorter than the corresponding distances determined on the ionic clusters. This effect is also observed on the second shell. For chloride, its first and second solvation shells are placed at average distances of 3.08 ± 0.02 and 4.21 ± 0.13 Å, respectively. Again, these values are smaller than those obtained from simulation of single ion systems and the contraction is more noticeable than for the protonic ions. The shorter distances observed is related to the simultaneous presence of the cation and the anion in the cluster leading to more compact hydration shells around them. The increase on temperature has a small effect on the average position of the hydration shells: it is <0.01 Å for the first shell and ∼0.02 Å for the second one.

The competition between the proton and chloride for the available water molecules, described in terms of their coordination numbers, can also be used to follow the charge separation with increasing cluster size. In Figure 6, the average distance between H^+ (the protonic moiety) and Cl^- shows that, for the small clusters ($n = 6-8$), the limited number of water molecules induces direct contact between the ions (CIP). The onset of ionic separation corresponds to the completion of the first shell around the Zundel ion and follows a trend that closely matches the growth of the second hydration shell of the protonated ion. At $n = 12$, the interaction between the ions is mediated on average by a single shell of water molecules. After a maximum average ionic separation of 4.40 Å ($n = 19$), there is a small reduction for clusters with 20 and 21 water molecules, mainly caused by the emergence of the clathrate-like structures in which the extended hydrogen bond network forms a two-dimensional layer that closes over itself; hence subsequent proton transfers do not necessarily result in further ion separation. An indication of the strong interplay between the ions and their solvation shells comes from the fact that the interionic distance does not show the same trend observed for the average maximum diameter of the clusters. Indeed, the average distance between the ions is always smaller than the average radius of the cluster. This strongly suggests that, although the protonic ion and chloride prefer to be located on the surface of ionic clusters, their simultaneous presence in small and medium-sized clusters does not allow them to migrate to the surface. In order to check which of the ions moves to the surface and which is solvated in the interior of the cluster, we calculated the average distance of the ions to the center of mass (COM) of the water cluster (chloride ion was not considered for finding the COM of the cluster). The data in Figure 7 confirm that the cationic form migrates to the surface of the cluster and the chloride ion moves from the surface of small clusters to the interior of clusters with

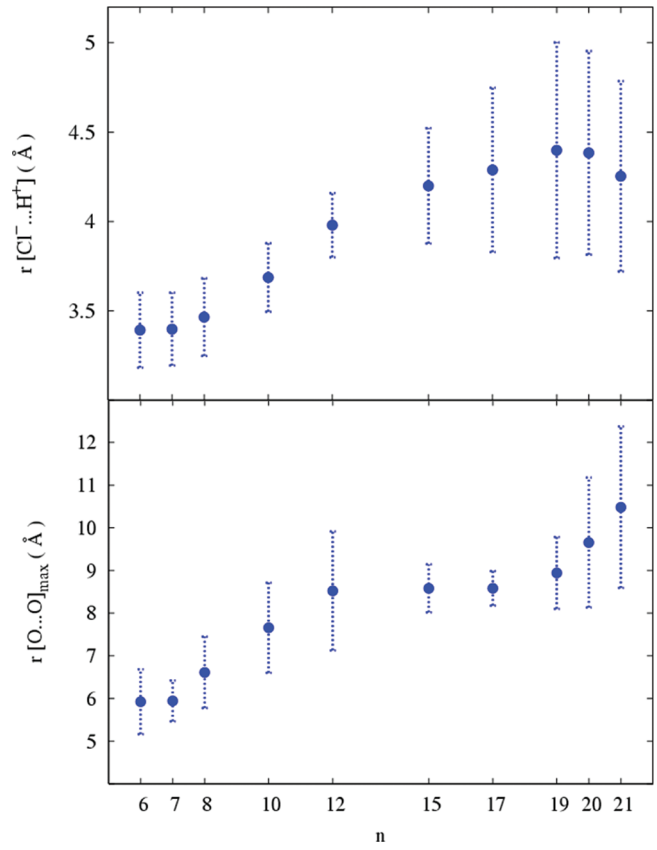

Figure 6. Average distance between the protonic species and the chloride ion (top panel) and maximum O···O distance in $HCl(H_2O)_n$ clusters (bottom panel).

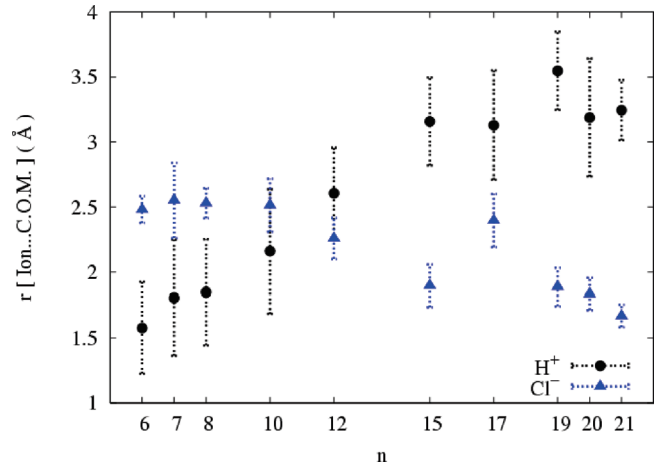

Figure 7. Average distance of ions to the center of mass in $Cl(H_2O)_n$ aggregates.

more than 12 water molecules. However, ions never achieve the maximum separation possible because they share at least one water molecule in their first solvation shell as shown in Figure 8. In these cluster sizes, the solvation of the ions is incomplete and no independently hydrated ions are formed; the SSIP state is the prevalent one. Furthermore, increasing the temperature leads to a slightly shorter value of the average interionic distances (0.2 Å). This effect is more pronounced for aggregates with $n \geq 12$, suggesting that the charge separation process has a small but nonnegligible dependence on the deformation of the hydrogen bond network.

It is clear that with 21 water molecules it is not possible to build two independent sets of solvation structures around the

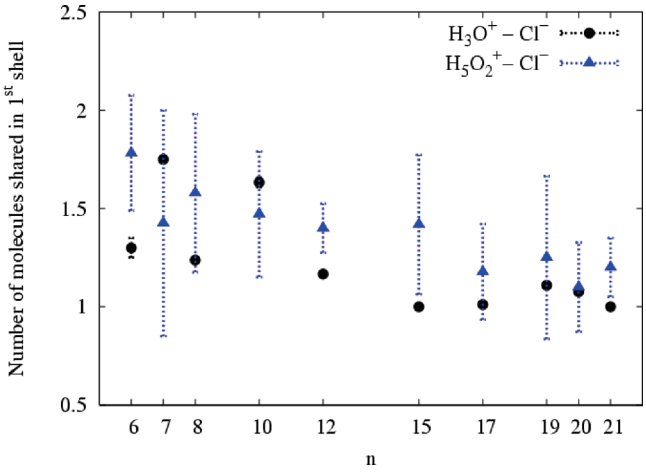

Figure 8. Average number of water molecules shared in first shell between protonated species and chloride in $HCl(H_2O)_n$ clusters.

ions. For that reason we calculated a 50 ps trajectory for the $HCl(H_2O)_{42}$ system. The average cation−anion distance in it was found to be 5.42 ± 0.17 Å, which represents an approximately 1 Å increase with respect to the 21 water molecule cluster. Again, it is observed that the protonic form migrates closer to the surface of the cluster than the chloride ion. The increase in water molecules available has a significant effect on the size of solvation shells. The number of water molecules in the first shell of the Zundel form goes from 3.6 ± 0.5 to 4.0 ± 0.0 and the effect is more pronounced for the anion: from 3.5 ± 0.9 to 5.1 ± 0.6 molecules. Second shells are also enlarged, with this effect being more noticeable around chloride in going up to 8.03 ± 1.0 molecules. We verified if there were still water molecules shared by the first solvation shells of the ions and found that this situation occurred in 72.2% of the trajectory compared to 93.5% of the 21 water molecule cluster. These results convey the idea that charge separation is indeed a slow process. In the following section we explore the reasons behind this finding.

C. Polarization and Charge Transfer around the Ions. Polarization and charge transfer are the two phenomena responsible for the strong correlation between the solvation shells and the ion displacements in the cluster. It is known that both polarization and charge transfer are accentuated in ionic hydrogen bonded complexes due to the enhanced electrostatic forces exerted on electrons.[5] Tuñon et al. showed that proton solvation induced a charge transfer from the solvent to the H_3O^+ or $H_5O_2^+$ ion[71] and an analogous situation can be expected to occur around the chloride ion. In order to assess the charge distribution in the cluster and its effects on the charge separation in these systems, we used the information coming from the semiempirical wave function. The polarization of the molecules in the cluster is evaluated in terms of the induced dipole moment. Using the Mulliken charges, the dipole moment of each molecule in the cluster was calculated as the vectorial sum of the products between atomic charges and its distances with respect to the center of mass of the molecule and then compared with the gas phase value computed in the same way. This procedure is known to underestimate the absolute value of the molecular dipolar moment; however, it gives the correct magnitude of the induced dipole.[72] In Table 3, the average relative induced dipole of the molecules in the first and second hydration shells is presented. The H_3O^+ induces the largest dipole moment in the molecules that surround it; the effect is more pronounced in the first shell than in the second. This latter is as polarized as the one around the $H_5O_2^+$ ion. Interestingly, the polarization occurring in medium-sized clusters is larger than for small clusters, but since all structures correspond to SSIP, it is clear that water molecules experience an enhanced polarizing field when they locate between both ions. When the same analysis is performed only for water molecules common to the first shell of chloride and the protonic form, it is found that such molecules display the largest induced dipole moment, 48−53%.

TABLE 3: Relative Induced Dipole Moment of Water Molecules in the Coordination Shells of Ions[a]

	H_3O^+	$H_5O_2^+$	Cl^-
	n = 6−12 (100 K)		
first shell	1.44 ± 0.02	1.40 ± 0.01	1.41 ± 0.01
second shell	1.36 ± 0.03	1.36 ± 0.02	1.41 ± 0.02
	n = 15−21 (100 K)		
first shell	1.48 ± 0.02	1.44 ± 0.02	1.44 ± 0.02
second shell	1.41 ± 0.01	1.39 ± 0.01	1.40 ± 0.01

[a] Values are relative to the gas phase value (0.974 D) calculated with the Mulliken charges and the PM3-MAIS predicted geometry as explained in the text.

The analysis of the charge distribution in these clusters allows looking at the charge transfer process occurring between the ions and their hydration shells. The net charge of each species was calculated as the sum of the Mulliken atomic charges. It is known that Mulliken charges calculated from semiempirical electronic distributions produce charge transfer trends among several hydrogen bonded complexes in good agreement with other methodologies.[73] Mulliken population analysis shows that H_3O^+ and $H_5O_2^+$ cations hold an average charge of 0.53 ± 0.02 and 0.61 ± 0.04 au, respectively. Interestingly, water molecules in the first solvation shell of H_3O^+ have an average charge of 0.06 au that closely matches the charge difference between both cations (0.07 au). Thus, the slight geometric change occurring during the continuous Eigen−Zundel interconversion process is not accompanied by a significant modification in the electronic density of the molecules involved.

The transference of electronic density from water molecules toward the cation generates a charge deficiency on its solvation shells. The first hydration shells around H_3O^+ and $H_5O_2^+$ ions exhibit a total average charge per molecule of 0.18 ± 0.03 and 0.13 ± 0.04 au, respectively, which is reduced by 60% in their second solvation shells. The ability of H_3O^+ to delocalize its charge among solvating molecules with respect to the Zundel cation concurs with a recent analysis on proton peripheral water molecules of structures extracted from bulk phase simulation.[19] The drop in the charge transfer on going from first shell to second shell corroborates its local character.

In Figure 9 we present the average charge of Cl^- in the clusters. If the solvation structure is small, the amount of charge transferred by the halide is more important than for the cases where the solvation structure is larger. This situation might be due to the fact that water molecules are better suited to transfer charge to the cation than the halide;[74,75] thus, only the cation first neighbors are involved in this transfer because they can accept charge from the anion. As the number of water molecules around the cation grows, the demand on charge from chloride diminishes. This situation is also responsible for the slow growth on the solvation shell around chloride.

D. Dynamic Behavior of the Proton in Neutral Clusters. The average lifetime of the protonated ion is calculated employing the direct count method.[8,9,47] Each configuration is inspected for determining the presence of H_3O^+ or $H_5O_2^+$; the occurrence of either changes the value of the corresponding

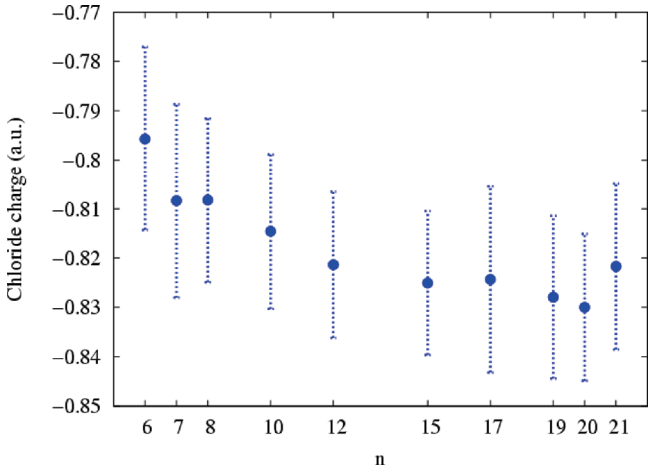

Figure 9. Average charge of chloride in $HCl(H_2O)_n$ clusters.

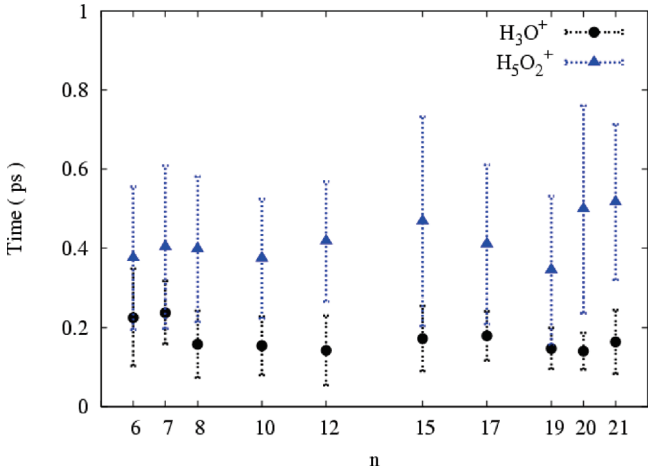

Figure 10. Average lifetime of the protonic forms defined as H_3O and H_5O_2 cations in $HCl(H_2O)_n$ clusters.

TABLE 4: Average Lifetime (fs) of Protonated Species in $HCl(H_2O)_n$ Clusters

cation	100 K	200 K
H_3O^+	234 ± 140	186 ± 75
$H_5O_2^+$	552 ± 290	355 ± 115

function, $E(i)$ or $Z(i)$, from 0 to 1. Isolated or adjacent detections of the protonated ion are considered as detection intervals. The average lifetime of each species is calculated as the mean length of the detection intervals. To soften the effect of fast structural deformations on average quantities, Sillanpää and Laasonen[47] implemented in their MD analysis the use of the filters t_c and t_l; we used the recommended values for $t_c = 50$ fs and $t_l = 200$ fs. The length of the detection intervals found throughout a particular trajectory depends on the geometric deformations of the protonated ion and the structural changes that occur in their solvation structures. These factors determine the interconversion between both cations and eventually drive the transference of proton through the hydrogen bond network. In Figure 10 we present the average lifetime of the cationic form as a function of the number of water molecules in the cluster. Table 4 shows the calculated global average lifetimes. The global average lifetime at 100 K for $H_5O_2^+$ is larger than the value calculated for H_3O^+. This difference can be explained by the fact that, in a polarized hydrogen bond network, the O···O distances that shape the proton potential well become shorter, favoring proton delocalization.[10,14] In such an environment, proton association to a single water molecule requires a more specific coordination shell composed mostly by three water molecules at similar O···O distances from the Eigen oxygen, but the constant movement of all atoms makes such a situation less probable. There is a small effect due to the cluster size: the Zundel form tends to longer lifetimes in larger clusters (6 fs per water molecule), while the opposite occurs for the H_3O^+ form. An interesting result is the large size of the fluctuations in this property: for both protonic forms they are approximately 50−60% of the average value. The size of these fluctuations are of the same magnitude as those calculated in HCl solutions.[47] Temperature has a large effect on average lifetimes: at 200 K, with a less interconnected network both cationic forms have shorter lifetimes. However, the effect is more pronounced for $H_5O_2^+$ (55%) than for H_3O^+ (25%). The size of the fluctuations around these average values is also diminished by ∼20%. Nonetheless, the average lifetime of the Zundel ion is still 1.9 times that of the H_3O^+ ion. Given the close connection between the proton transfer events and lifetimes of protonic species, it is convenient to notice that our estimation of the latter coincides with characteristic times calculated for proton transference near the surface of aggregates $H^+(H_2O)_{64}$,[76] but it is smaller compared to proton jumps toward the interior of those clusters ($\sim 10^3$ fs). A preliminary estimation of the proton transfer frequency in the $HCl(H_2O)_{20}$ cluster showed that proton jumps occur within an $\sim 10^3$ fs interval, in agreement with early estimations from molecular simulations of the cluster $H^+(H_2O)_{21}$;[69] however, a more systematic analysis is needed to assess the multiple effects involved in the transfer.

IV. Conclusions

We have shown that the semiempirical PM3-MAIS model for HCl in water produces results in excellent agreement with those coming from more refined methodologies. Due to its affordable computational cost, the long trajectories produced for studying the HCl dissociation in water clusters led to a detailed description of the ionic hydration process that follows the initial reaction. The cationic ions compete more successfully for hydration than the anion because both protonic forms end up with an almost complete second solvation shell and Cl^- ends with a partial solvation in the interior of the largest studied clusters. Nonetheless, the position and size of the first solvation shell closely resembles the one derived from neutron diffraction experiments of concentrated solutions, and the anisotropy theoretically predicted for it. The strong correlation between hydration structures around the ions prevents an independent set of hydration structures for them. As a consequence, most of the studied clusters produced ionic pairs separated by one water molecule. Interestingly, the charge transfer becomes very important for the first hydration shell of both ions and remains well localized in this zone; however, it is important to keep in mind that although our results are in excellent agreement with those coming from ab initio or density functional theory calculations, they were derived from a minimal basis set in which polarization effects are certainly underestimated. The vast amount of data analyzed for these systems confirms that the average lifetime of the Zundel cation is almost twice that of the H_3O^+ ion. The structural features found for the solvation of this ion suggest the possibility of entropic factors behind the prevalence of this protonic form. Another interesting finding is the fact that the formation of the Eigen complex ($H_9O_4^+$) does not depend on the amount of water molecules available in the cluster, although the fluctuations around its average lifetime are strongly correlated with the size of the cluster. The temperature effect on local and global structural properties seems to be small,

but it is quite obvious that changes in the water network can strongly modify cationic lifetimes.

Acknowledgment. This work was supported by CONACYT Grant 3835-E. O.I.A.F. received a CONACYT scholarship 170276. We would like to express our gratitude to Minhhuy Hô, Thomas Buhse, and Humberto Saint Martin for many fruitful discussions and to Manuel Ruiz-López and Iván Ortega-Blake for their valuable suggestions.

Supporting Information Available: Figures showing O−O and Cl−O radial distribution functions for the $HCl(H_2O)_{20}$ cluster calculated for 10 trajectories corresponding to 400 ps at 100 K. This material is available free of charge via the Internet at http://pubs.acs.org.

References and Notes

(1) Niedner-Schatteburg, G.; Bondybey, V. *Chem. Rev.* **2000**, *100*, 4059.
(2) Chang, H.-C.; Wu, C.-C.; Kuo, J.-L. *Int. Rev. Phys. Chem.* **2005**, *24*, 553.
(3) Seinfeld, J. H.; Pandis, S. P. *Atmospheric Chemistry and Physics*; John Wiley & Sons, Inc.: New York, 1998.
(4) Zidi, Z. S. *J. Chem. Phys.* **2005**, *123*, 064309.
(5) Meot-Ner, M. *Chem. Rev.* **2005**, *105*, 213.
(6) Buch, V.; Sadlej, J.; Aytemiz-Uras, N.; Devlin, J. P. *J. Phys. Chem. A* **2002**, *106*, 9374.
(7) Yamaguchi, S.; Kudoh, S.; Okada, Y.; Orii, T.; Takeuchi, K.; Ichikawa, T.; Nakai, H. *J. Phys. Chem. A* **2003**, *107*, 10904.
(8) Agmon, N. *Chem. Phys. Lett.* **1995**, *244*, 456.
(9) Tuckerman, M.; Laasonen, K.; Sprik, M.; Parrinello, M. *J. Chem. Phys.* **1995**, *103*, 150.
(10) Marx, D.; Tuckerman, M. E.; Hutter, J.; Parrinello, M. *Nature* **1999**, *397*, 601.
(11) Sadeghi, R. R.; Cheng, H. P. *J. Chem. Phys.* **1999**, *111*, 2086.
(12) Schmitt, U. W.; Voth, G. A. *J. Chem. Phys.* **1999**, *111*, 9361.
(13) Jiang, J. C.; Wang, Y. S.; Chang, H. C.; Lin, S. H.; Lee, Y. T.; Niedner-Schatteburg, G.; Chang, H. C. *J. Am. Chem. Soc.* **2000**, *122*, 1398.
(14) Marx, D. *ChemPhysChem* **2006**, *7*, 1849.
(15) Vener, M. V.; Librovich, N. B. *Int. Rev. Phys. Chem.* **2009**, *28*, 407.
(16) Zundel, G.; Metzer, H. *Z. Phys. Chem. (Munich)* **1968**, 58.
(17) Eigen, M. *Angew. Chem., Int. Ed. Engl.* **1964**, *3*, 1.
(18) Cavalleri, M.; Naslund, L. A.; Edwards, D. C.; Wernet, P.; Ogasawara, H.; Myneni, S.; Ojamae, L.; Odelius, M.; Nilsson, A.; Pettersson, L. G. M. *J. Chem. Phys.* **2006**, *124*, 194508.
(19) Swanson, J. M. J.; Simons, J. *J. Phys. Chem. B* **2009**, *113*, 5149.
(20) Combariza, J. E.; Kestner, N. R.; Jortner, J. *J. Chem. Phys.* **1994**, *100*, 2851.
(21) Kemp, D. D.; Gordon, M. S. *J. Phys. Chem. A* **2005**, *109*, 7688.
(22) Bergstrom, P. A.; Lindgren, J.; Kristiansson, O. *J. Phys. Chem.* **1991**, *95*, 8575.
(23) Markovich, G.; Pollack, S.; Giniger, R.; Cheshnovsky, O. *J. Chem. Phys.* **1994**, *101*, 9344.
(24) Ayala, R.; Martinez, J. M.; Pappalardo, R. R.; Marcos, E. S. *J. Chem. Phys.* **2004**, *121*, 7269.
(25) Likholyot, A.; Hovey, J. K.; Seward, T. M. *Geochim. Cosmochim. Acta* **2005**, *69*, 2949.
(26) Dang, L. X.; Smith, D. E. *J. Chem. Phys.* **1993**, *99*, 6950.
(27) Stuart, S. J.; Berne, B. J. *J. Phys. Chem.* **1996**, *100*, 11934.
(28) Petersen, C. P.; Gordon, M. S. *J. Phys. Chem. A* **1999**, *103*, 4162.
(29) Tobias, D. J.; Jungwirth, P.; Parrinello, M. *J. Chem. Phys.* **2001**, *114*, 7036.
(30) Yoo, S.; Lei, Y. A.; Zeng, X. C. *J. Chem. Phys.* **2003**, *119*, 6083.
(31) Herce, D. H.; Perera, L.; Darden, T. A.; Sagui, C. *J. Chem. Phys.* **2005**, 122.
(32) Wick, C. A.; Xantheas, S. S. *J. Phys. Chem. B* **2009**, *113*, 4141.
(33) Peslherbe, G. H.; Ladanyi, B. M.; Hynes, J. T. *J. Phys. Chem. A* **2000**, *104*, 4533.
(34) Lee, C. T.; Sosa, C.; Planas, M.; Novoa, J. J. *J. Chem. Phys.* **1996**, *104*, 7081.
(35) Ando, K.; Hynes, J. T. *J. Phys. Chem. B* **1997**, *101*, 10464.
(36) Milet, A.; Struniewicz, C.; Moszynski, R.; Wormer, P. E. S. *J. Chem. Phys.* **2001**, *115*, 349.
(37) Weimann, M.; Farnik, M.; Suhm, M. A. *Phys. Chem. Chem. Phys.* **2002**, *4*, 3933.
(38) Calatayud, M.; Courmier, D.; Minot, C. *Chem. Phys. Lett.* **2003**, *369*, 287.
(39) Botti, A.; Bruni, F.; Imberti, S.; Ricci, M. A.; Soper, A. K. *J. Chem. Phys.* **2004**, *121*, 7840.
(40) Odde, S.; Mhin, B. J.; Lee, S.; Lee, H. M.; Kim, K. S. *J. Chem. Phys.* **2004**, *120*, 9524.
(41) Shevkunov, S. V. *Colloid J.* **2004**, *66*, 216.
(42) Parent, P.; Laffon, C. *J. Phys. Chem. B* **2005**, *109*, 1547.
(43) Buch, V.; Dubrovskiy, A.; Mohamed, F.; Parrinello, M.; Sadlej, J.; Hammerich, A. D.; Devlin, J. P. *J. Phys. Chem. A* **2008**, *112*, 2144.
(44) Lee, H. S.; Tuckerman, M. E. *J. Phys. Chem. A* **2009**, *113*, 2144.
(45) Svanberg, M.; Pettersson, J. B. C.; Bolton, K. *J. Phys. Chem. A* **2000**, *104*, 5787.
(46) Ardura, D.; Donaldson, D. J. *Phys. Chem. Chem. Phys.* **2009**, *11*, 857.
(47) Sillanpää, A. J.; Laasonen, K. *Phys. Chem. Chem. Phys.* **2004**, *6*, 555.
(48) Bondibey, V. E.; Beyer, M. K. *Int. Rev. Phys. Chem.* **2001**, *21*, 277.
(49) Huneycutt, A. J.; Saykally, R. J. *Science* **2003**, *299*, 1329.
(50) Arillo-Flores, O. I.; Ruiz-López, M. F.; Bernal-Uruchurtu, M. I. *Theor. Chem. Acc.* **2007**, *118*, 425.
(51) Takayanagi, T.; Takahashi, K.; Kakizaki, A.; Shiga, M.; Tachikawa, M. *Chem. Phys.* **2009**, *358*, 196.
(52) Rinaldi, D.; Hoggan, P. E.; Cartier, A. *QCPE Bull.* **1989**, *584a*, 128.
(53) Allen, M. P.; Tildesley, D. J. *Computer Simulation of Liquids*; Oxford Science Publications: Oxford, U.K., 1994.
(54) Maheshwary, S.; Patel, N.; Sathyamurthy, N.; Kulkarni, A. D.; Gadre, S. R. *J. Phys. Chem. A* **2001**, *105*, 10525.
(55) Hodges, M. P.; Wales, D. J. *Chem. Phys. Lett.* **2000**, *324*, 279.
(56) Geissler, P. L.; Dellago, C.; Chandler, D.; Hutter, J.; Parrinello, M. *Science* **2001**, *291*, 2121.
(57) Voloshin, V. P.; Naberukhin, Y. I. *J. Struct. Chem.* **2009**, *50*, 78.
(58) Nakahara, M.; Wakai, C. *J. Mol. Liq.* **1995**, *65−66*, 149.
(59) Devlin, J. P.; Uras, N.; Sadlej, J.; Buch, V. *Nature* **2002**, *417*, 269.
(60) Botti, A.; Bruni, F.; Ricci, M. A.; Soper, A. K. *J. Chem. Phys.* **2006**, *125*, 014508.
(61) Kuo, J. L.; Klein, M. L. *J. Chem. Phys.* **2005**, *122*, 24516.
(62) Botti, A.; Bruni, F.; Imberti, S.; Ricci, M. A.; Soper, A. K. *J. Mol. Liq.* **2005**, *117*, 77.
(63) Burnham, C. J.; Petersen, M. K.; Day, T. J. F.; Iyengar, S. S.; Voth, G. A. *J. Chem. Phys.* **2006**, *124*, 024327.
(64) Soper, A. K.; Weckström, K. *Biophys. Chem.* **2006**, *124*, 180.
(65) Heuft, J. M.; Meijer, E. J. *J. Chem. Phys.* **2003**, *119*, 11788.
(66) Bernal-Uruchurtu, M. I.; Ruiz-López, M. F. In *Beyond Standard Quantum Chemistry: Applications From Gas To Condensed Phases*; Hernández-Lamoneda, R., Ed.; Transworld Research Network: Kerala, India, 2007; p 65.
(67) Parthasarathi, R.; Subramanian, V.; Sathyamurthy, N. *J. Phys. Chem. A* **2007**, *111*, 13287.
(68) Shin, J. W.; Hammer, N. I.; Diken, E. G.; Johnson, M. A.; Walters, R. S.; Jaeger, T. D.; Duncan, M. A.; Christie, R. A.; Jordan, K. D. *Science* **2004**, *304*, 1137.
(69) Laasonen, K.; Klein, M. L. *J. Am. Chem. Soc.* **1994**, *116*, 11620.
(70) Lagutschenkov, A.; Fanourgakis, G. S.; Niedner-Schatteburg, G.; Xantheas, S. S. *J. Chem. Phys.* **2005**, 122.
(71) Tuñon, I.; Silla, E.; Bertran, J. *J. Phys. Chem.* **1993**, *97*, 5547.
(72) Monard, G.; Bernal-Uruchurtu, M. I.; van der Vaart, A.; Merz, K. M. J.; Ruiz-López, M. F. *J. Phys. Chem. A* **2005**, *109*, 3425.
(73) van der Vaart, A.; Merz, K. M. J. *J. Chem. Phys.* **2002**, *116*, 7380.
(74) Rustam, Z. K.; Alexis, T. B.; Martin, H.-G. *Chem.—Eur. J.* **2009**, *15*, 851.
(75) Nilsson, A.; Ogasawara, H.; Cavalleri, M.; Nordlund, D.; Nyberg, M.; Wernet, P.; Pettersson, L. G. M. *J. Chem. Phys.* **2005**, *122*, 154505.
(76) Kobayashi, C.; Iwahashi, K.; Saito, S.; Ohmine, I. *J. Chem. Phys.* **1996**, *105*, 6358.

JP101803R